Adaptation of Lateral-Line Inspired Force Compensation Algorithms for Underactuated Marine Vehicles

Michael Krieg[1], and Kamran Mohseni[1,2,3]

***Abstract*— This paper investigates control methodologies for underactuated marine vehicles in chaotic fluid environments. Recent studies in our group have shown excellent potential for a novel control methodology inspired by fish lateral line sensory systems, whereby a vehicle measures exact hydrodynamic forces acting on it via a distributed pressure sensor array, and then applies control forces to instantaneously compensate for measured fluid forces. However, the new technique requires that the vehicle is capable of producing forces/torques in all degrees of freedom independently, and unfortunately most marine vehicles are underactuated, in that forward and lateral forces are coupled to each other. Here we develop a new motion control algorithm, which is a modified line-of-sight heading algorithm, to allow these vehicles to utilize hydrodynamic force measurements and improve position tracking. We demonstrate the effectiveness of the derived control strategy by creating a simulation of an underactuated vehicle in the presence of fluid disturbances, under both a standard line-of-site heading algorithm and the one defined here. We found that the new motion controller significantly reduces position tracking error, even by more than 50% in some cases. In general the new control shows the most benefit for cases with large disturbance amplitudes and lower disturbance frequencies.**

I. INTRODUCTION

Fluid disturbances, especially in regions like littorals and coastal surf zones, can be not only significant, but difficult to model. This makes position tracking extremely difficult, despite the fact that accurate positioning is often more critical in these regions due to a high density of obstacles and other threats. The substantial impact that ocean currents and waves have on marine vehicles has long been a critical problem for the control designers of those vehicles [1].

Typically hydrodynamic forces are modeled in terms of the relative state of the vehicle with respect to the local fluid environment [2]. As such, fluid forces are categorized into drag or viscous forces, that scale with the the relative vehicle velocity, and added mass forces, that scale with relative vehicle acceleration. Inherent in this type of hydrodynamic force modeling is the assumption that the surrounding fluid has a single uniform velocity and that the vehicle moves with a velocity relative to that. There are several issues with this type of approach. From a physical standpoint, it should be pointed out that there are no such forces as drag and added mass, the interaction between a vehicle and the surrounding takes place through the distribution of pressure and shear stress on the vehicle body, which are only broken down into parts that scale like viscosity and parts that scale like inertia for convenience. Not to mention the fact that as flows become more chaotic and the surrounding flow can no longer be considered uniform, the entire model breaks down. From a practical standpoint, the relative vehicle velocity is also difficult to measure since the fluid very near the body is affected by vehicle motion. Furthermore, the drag terms are non-linear functions of vehicle velocity, which makes them difficult to handle with standard controllers.

There have been several complicated control techniques employed to alleviate these issues such as disturbance velocity estimators [3], sliding mode [4], [5], [6] and adaptive [7], [8] controllers, Kalman filter based velocity/disturbance estimators [9], [10], and neural network or machine learning based estimators [11], [12]. These techniques have varying degrees of success, but they ignore the critical issue, which is that the hydrodynamic forces are functions of an abundance of fluid environmental states in addition to the vehicle states. If there is no unique solution for hydrodynamic forces with respect to a given set of vehicle inertial sensor measurements, they cannot be calculated, no matter how well the adaptive models or learning algorithms are designed.

The limitations of the formulation of hydrodynamic forces with respect to vehicle velocity motivated us to avoid such modeling altogether; and instead focus on measuring hydrodynamic forces acting on a freely swimming AUV in real time using a distributed sensory system inspired by the lateral line system in fish [13], [14], [15]. By measuring the forces and moments directly, a controller can be designed to oppose for these forces, in real time, compensating for the disturbance before it has a chance to displace the vehicle. This methodology also decouples the vehicle states from the fluid states, effectively reducing the control problem to that of the control of a rigid body in a vacuum, allowing the use of classical control theories and gain tuning methodologies. In recent studies, we have not only shown the effectiveness of the lateral line inspired sensory system in measuring hydrodynamic forces [14], we have also shown that the instantaneous compensation of fluid forces significantly decreases position tracking errors both in simulation [13] and through empirical testing on a freely swimming underwater vehicle [15]. The empirical testing showed that the new motion control algorithm enabled by the bioinspired sensory system decreased position errors by 72% for the vehicle with full control authority.

Issues with Underactuated Vehicles - The measured force

University of Florida, P.O. Box 116250, Gainesville, FL 32611
[1]Department of Mechanical and Aerospace Engineering
[2]Department of Electrical and Computer Engineering
[3]Institute for Networked Autonomous Systems email: mohseni@ufl.edu
Digital Object Identifier (DOI): see top of this page.

compensation technique [13], [14], [15] assumes that the surface/underwater vehicle is fully controllable, meaning that it is capable of providing independent control forces/torques in each of the active degrees of freedom. Under this assumption the vehicle is able to provide control forces exactly equal and opposite to the hydrodynamic forces, negating their effect on vehicle motion, and provide additional forces to follow the desired trajectory.

Typically, in order to simplify their design, surface vessels are equipped with a single thruster for forward propulsion, and have some means of directional control over that thruster via either a rudder or some mechanism for vectoring the thruster. This corresponds to an underactuated system because sway forces and yaw torques are coupled to the surge force. This means that lateral hydrodynamic disturbances cannot be compensated without affecting the forward trajectory. In this paper we define a new control strategy for underactuated vehicles in order to utilize the disturbance force measurements by modifying standard line-of-sight heading algorithms and simulate the performance on a virtual vehicle to validate the new algorithm. We start off by defining the vehicle dynamics used for the simulation, and derive the new control strategy in section II. The details of the simulation are provided in section III, and then analyze the results in section IV.

II. VEHICLE MODELING AND CONTROL

In this section we lay out the vehicle governing dynamics and define control laws that will be used to simulate position tracking performance. As part of this simulation, the hydrodynamic forces must be modeled. For the sake of simplicity, we will model these forces in terms of vehicle relative velocities. Even though these models break down for complex flows, as was just discussed, it should be noted that the controller is unaffected by the complexity of the simulation hydrodynamic force model. From the controller perspective fluid forces are being measured directly and used to adjust heading/thrust. Therefore, the complexity of the simulation force modeling does not affect the controller performance. For this preliminary study, we will impose unsteady, but uniform, disturbances and model forces through drag and added mass terms, showing the controller response framework. However, the algorithm can be applied to any form of disturbance, provided that the distributed sensory system measures those force accurately.

A. Underactuated Vehicle Dynamics

For the purposes of this study, the vehicle will only be allowed to move within the lateral plane, i.e. the vehicle is free to move in surge, sway, and yaw, but restricted in heave, roll, and pitch directions. This simplification will allow concepts related to the heading control algorithm to be more easily conceptualized, without loss of generality to unrestrained six degree-of-freedom (DOF) vehicles. The vehicle and corresponding coordinate definitions are depicted in figure 1. The inertial position/orientation within the lateral plane is given by, $\eta = [x, y, \Psi]^T$, whereas the velocity vector in the body fixed frame is denoted, $\nu = [u, v, r]^T$. There is no physical meaning for the integral of the body fixed velocity.

The governing dynamics of this vehicle are defined,

$$\begin{aligned} \dot{\eta} &= J\nu \,, \\ M\dot{\nu} &= \tau_C + \tau_H \,, \\ J &= \begin{bmatrix} \cos\Psi & -\sin\Psi & 0 \\ \sin\Psi & \cos\Psi & 0 \\ 0 & 0 & 1 \end{bmatrix} \end{aligned} \tag{1}$$

where M is the mass/inertia matrix $M = diag\{m, m, I_Z\}$, τ_C are the control forces and τ_H are the hydrodynamic forces acting on the vehicle.

The goal of this study is to adapt a novel control methodology to be used on underactuated marine vehicles, meaning that they cannot generate forces in the surge, sway, and yaw directions independently of one another. This is an extremely common occurrence for both submerged and surface vessels, that typically use one primary propulsor which is either gimbled to vector thrust, or used in conjunction with rudders or other control surfaces. As the most basic representation we will parameterize the control forces by a propulsor force, T, and angle, α, so that

$$\tau_C = [T\cos\alpha, T\sin\alpha, -T\sin\alpha, d_{\text{prop}}]^T \,, \tag{2}$$

see figure 1. Admittedly, this definition fits more easily with gimbled thrusters, but can also be applied to rudder vehicles by defining and equivalent thrust/angle associated with a given rudder deflection.

The hydrodynamic forces acting on the vehicle will be simulated with respect to vehicle relative velocities, in the standard fashion [2],

$$\tau_H = -M_A\dot{\nu}_{\text{rel}} - N\nu_{\text{rel}} \,, \tag{3}$$

where ν_{rel} is the body fixed vehicle velocity relative to the surrounding fluid velocity, M_A is the added mass matrix of the vehicle, N is the combined drag and Coriolis/centripetal matrix, and all restoring forces have been neglected since the vehicle only operates in the lateral plane.

The coefficients used for the virtual vehicle in this study correspond to an autonomous surface vessel and are summarized in table I. Specifically, the surface vessel is a high speed recreational 2 person recreational craft, which has a large range of thrust angles. It should be noted that the model for hydrodynamic forces has been linearized about trim conditions for simplicity since an exact representation of the hydrodynamic forces is not as important to this study as the vehicle response to those forces.

The vehicle is subjected to an oscillating background flow to represent ocean current disturbances. The background flow is created in the global X direction, and oscillates with frequency ω (Hz) and amplitude A, so that

$$\dot{x}_{\text{dist}} = A\sin(2\pi\omega t) \,. \tag{4}$$

The control forces, τ_C, are determined by the vehicle control algorithms, which is defined in the next section. For this preliminary investigation we will consider the thruster to

TABLE I

SUMMARY OF VEHICLE HYDRODYNAMIC COEFFICIENTS. ALL COEFFICIENTS NOT LISTED IN THIS TABLE ARE SET TO ZERO.

i	j	M	M_A	N
1	1	650	59	48.3
2	2	650	103	116.4
2	3	0	0	1.9
3	2	0	0	-1.9
3	3	429	0	9.3

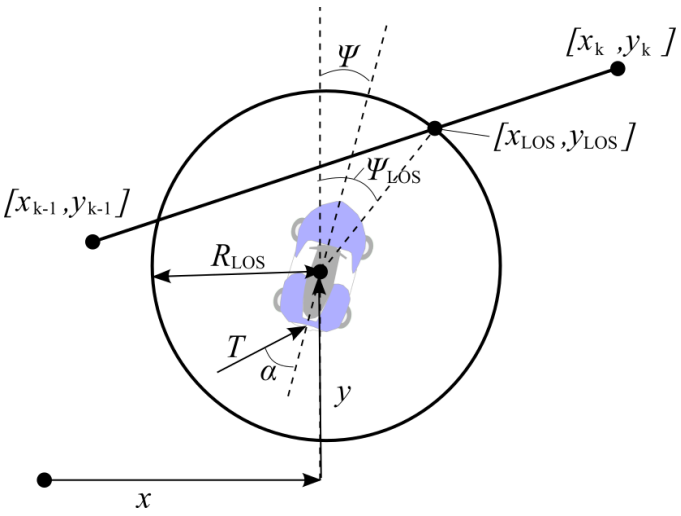

Fig. 1. Schematic diagram of the line-of-sight (LOS) heading algorithms. Under this methodology desired heading is set to be the intersection of a waypoint path segment and a circle of some given radius around the vehicle.

have a maximum thrust vectoring angle, $-65^\circ \leq \alpha \leq 65^\circ$, but we will not impose any limit on the magnitude of the thrust.

B. Adapted Force Compensation Algorithm

As was mentioned in the introduction, an underactuated marine vehicle cannot create surge and sway forces independently, since the single propulsor couples the two. Therefore, hydrodynamic forces measured by a bioinspired distributed sensory system [14] cannot be directly compensated to improve position tracking as is done in [13], [15]. However, the hydrodynamic force measurements can still be used to improve position tracking by including adjustments to traditional heading controllers used for underactuated marine vehicles. This section gives a summary of a standard heading controller, and provides details of how it can be adapted to include hydrodynamic force measurements and improve tracking stability.

In general, underactuated surface vessels track a desired heading and forward velocity, where corrections are made to the heading due to sway displacement allowing for lateral tracking stability. One common method for determining a desired heading is to implement a line-of-sight (LOS) algorithm with a series of desired waypoints, which provides some indirect compensation for errors in the lateral position/velocity [16], [17]. The concept of the LOS heading control is shown in figure 1, where $[x_k, y_k]$ is the current waypoint, the index $k-1$ refers to the previous waypoint, Ψ is the current heading of the vehicle at position $[x, y]$. Given some radius around the vehicle R_{LOS}, a desired heading Ψ_{LOS} can be defined by the intersection of the radius and the waypoint trajectory. Therefore if the vehicle lies on the desired trajectory, the desired heading just points to the next waypoint, however, as the lateral error grows the desired heading will be adjusted to correct for this error. By adjusting R_{LOS} the designer can shift the balance between smooth vehicle motion and reduced lateral errors. Hence the desired heading can be calculated from the following equations summarizing the geometric constraints,

$$\begin{aligned} \Psi_{LOS} &= \text{atan2}\left(y_{LOS}, x_{LOS}\right) , \\ R_{LOS} &= \left(y_{LOS} - y\right)^2 + \left(x_{LOS} - x\right)^2 , \\ \frac{y_{LOS} - y_{k-1}}{x_{LOS} - x_{k-1}} &= \frac{y_k - y_{k-1}}{x_k - x_{k-1}} . \end{aligned} \tag{5}$$

The desired forward velocity is usually just defined as some constant, $u_d = const$, associated with the optimal thruster parameters.

Once a desired heading and forward velocity have been determined we need to design a controller to drive the vehicle to these desired values, by vectoring the main thruster at some angle, α, and throttling the force T. There are multiple techniques with varying degrees of complexity for this control design. Model based back-stepping methods [2] produce good results, but assume that fluid disturbances are very large compared to the vehicle size (i.e. it experiences a uniform relative fluid velocity). This is not the case in complex environments like coastal regions and littorals, so we will restrict this first level analysis to simpler PD controllers for α and T [16], [17], based on feedback of heading error, $\tilde{\Psi} = \Psi_d - \Psi$, and forward velocity error, $\tilde{u} = u_d - u$, respectively,

$$\alpha = k_{\Psi p}\tilde{\Psi} + k_{\Psi d}\dot{\tilde{\Psi}} , \quad T = \frac{k_{up}\tilde{u} + k_{ud}\dot{\tilde{u}}}{\cos(\alpha)} . \tag{6}$$

When it comes to compensating for disturbances, an underactuated vehicle cannot simultaneously compensate for hydrodynamic forces/torques in the surge, sway, and yaw directions. Instead, as is similar to the vehicle controller methodology, we will add additional terms to the thruster controller to compensate for hydrodynamic yaw torque and surge force, and an additional term is added to the desired heading term to compensate for the sway force. We start by defining an additional control term τ_{DC}, which is (2) evaluated at α_{DC} and T_{DC}, and set the surge force and yaw torque equal and opposite to the respective measured hydrodynamic forces in those directions F_u and τ_r. Adding T_{DC} and α_{DC} to (6) yields the disturbance compensation thruster controller,

$$\begin{aligned} \alpha &= atan\left(\frac{-\tau_r}{-F_u d_{prop}}\right) + k_{\Psi p}\tilde{\Psi} + k_{\Psi d}\dot{\tilde{\Psi}} , \\ T &= \sqrt{F_u^2 + \left(\frac{\tau_r}{d_{prop}}\right)^2} + \frac{k_{up}\tilde{u} + k_{ud}\dot{\tilde{u}}}{\cos(\alpha)} . \end{aligned} \tag{7}$$

The correction to the heading is slightly more complicated than a simple force balance. If a sway force is acting on a vehicle, the sway velocity, v, will build up cumulatively over time until either the fluid viscous forces reach equilibrium with the disturbance force or the disturbance force dissipates. Therefore, we need a heading correction term that similarly builds up cumulatively the longer a vehicle is exposed to a disturbance force. For this algorithm consider a vehicle exposed to a sway disturbance force F_v without any control action taken. Over the time span in between control loop iterations the vehicle will have been displaced $F_v/\left(2mf_C^2\right)$, where f_C is the frequency of the control loop. Over the same period of time, assuming the vehicle is traveling at the desired forward speed, it will have traveled a distance u_d/f_C. Thus, a differential heading adjustment can be defined which will result in an equal and opposite vehicle sway displacement over this differential time step,

$$d\Psi_{DC} = \text{atan}\left(\frac{-F_v}{2mu_d f_C}\right). \tag{8}$$

Finally, by integrating over time we get a heading correction for disturbance compensation that is added to the LOS heading angle,

$$\Psi_d = \Psi_{LOS} + \int_0^t \text{atan}\left(\frac{-F_v(t)}{2mu_d f_C}\right) dt\,. \tag{9}$$

III. SIMULATION DETAILS

In order to analyze the efficacy of the proposed motion control algorithm, we simulate the response of a virtual underactuated vehicle in an environment with an oscillating background flow using a Matlab code and measure the position/velocity tracking performance. At the onset of the simulation the user provides characteristic parameters of the vehicle, table I, a set of waypoints defining the desired trajectory, the control loop iteration frequency, f_C, and the magnitude and frequency of the background flow, A and ω.

At each control loop iteration, the simulation calculates a desired heading, Ψ_d, a thruster magnitude, T, and a thrust vector angle α. For the standard controller case, the desired heading is set to Ψ_{LOS}, and the thrust control terms are calculated from (6). For the disturbance compensation case the desired heading is calculated from (7) and the thruster terms are calculated from (4). The resulting control forces (2) are then plugged into the vehicle dynamics (1) and the vehicle trajectory over the timespan in between control loop iterations is integrated using Matlab's ODE45 integrator updating hydrodynamic forces (3) at each step of the numerical integration. The trajectory is integrated in between control loop iterations, so that the trajectory will remain accurate even for very low control loop frequencies.

There two predefined waypoint trajectories used in this study for different purposes, which will be referred to as WP1 and WP2. WP1 consists of of waypoints forming a straight line parallel to the inertial y axis, and hence perpendicular to the fluid disturbance velocity. This trajectory is used to make quantitative comparisons between the different control strategies. The second waypoint trajectory, WP2, has 3 sections, first parallel to the x axis, then running diagonally, then parallel to the y axis. WP2 is a more complex desired trajectory, which allows for a more qualitative representation of controller performance.

For a representative disturbance case (A = 3 m/s, ω = 0.01 Hz), the vehicle motion was recorded while attempting to follow WP1 using a range of values for the control gains $k_{\Psi p}$, $k_{\Psi d}$, k_{up}, k_{ud}. For each control strategy we then selected the combination of control gains that minimized the overall position tracking error for this representative case. For the standard LOS controller, the optimal control gains are $k_{\Psi p} = 3.5$, $k_{\Psi d} = 0.87$, $k_{up} = 120$, $k_{ud} = 60$. For the disturbance compensation adjusted LOS controller, the optimal control gains are $k_{\Psi p} = 4.2$, $k_{\Psi d} = 2.3$, $k_{up} = 120$, $k_{ud} = 60$. Although these control gains will not be exactly optimal for all disturbance conditions, they provide a good baseline for the comparison of different control methodologies. For cases tested in this simulation we set the desired forward velocity to $u_d = 5$ m/s and the LOS radius to 40 m.

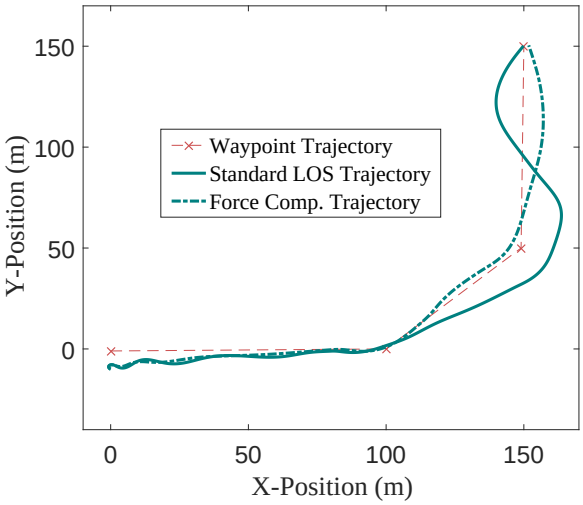

Fig. 2. Position tracking stability of the virtual underactuated vehicle for an example mission trajectory (WP2) using both the standard LOS heading algorithm and the LOS heading algorithms with disturbance compensation adjustments. The background flow oscillates in the x direction with an amplitude of 3 m/s and a frequency of 0.03 Hz.

IV. TRACKING STABILITY: SIMULATION RESULTS

The Underactuated marine vehicle behavior was simulated as described in section III while attempting to follow multiple waypoint trajectories using both a standard LOS heading control algorithm and a LOS heading algorithm with additional disturbance force compensation terms, as defined in section II-B. Figure 2 shows the trajectory of the vehicle for the two different control strategies while attempting to track WP2 in the presence of an oscillating background flow (A = 3 m/s, ω = 0.03 Hz). It can be seen that the disturbance force compensating controller performs significantly better at tracking the desired trajectory. As would be expected there is little difference between the position tracking of the

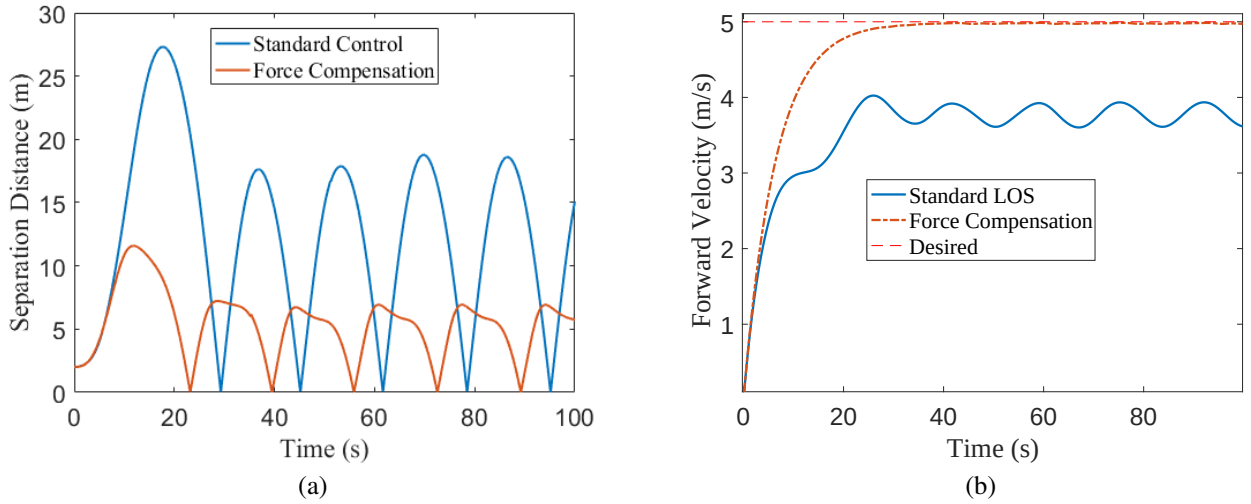

Fig. 3. Instantaneous error in position and velocity tracking for the vehicle subject to disturbances with amplitude A = 5 m/s and frequency ω = 0.03 Hz. (a) shows the separation distance from the desired path during the run, and (b) shows the forward velocity during the run for both control strategies.

two strategies when the vehicle is moving parallel to the disturbance flow, but there is a difference in the forward velocity tracking as will be discussed later. Over the other legs of the trajectory the standard LOS controller suffers from significant displacement before the heading is steered back towards the desired path.

For a more quantitative analysis we ran the simulation of the vehicle attempting to follow WP1 using both control strategies for a range of background disturbance velocity amplitudes and a disturbance frequency of 0.03 Hz. For each case the simulation was run until the vehicle reached the final waypoint, at time t_f, and the separation distance between the vehicle position and the desired path, $\delta(t)$ was measured at every point in time. The total position error of each run is calculated as the root mean square of the separation distance, $e = \sqrt{\int_0^{t_f} \delta^2 \, dt / t_f}$.

Figure 3 shows the separation distance and forward velocity for both control strategies for the case where A = 5 m/s and ω = 0.01 Hz. It can be seen that the disturbance force compensation algorithm results in a lower maximum separation distance being reached for each disturbance cycle. For this case the disturbance compensation strategy reduces the total position tracking error by 52% compared to the standard LOS heading controller. The vehicle forward velocity for both cases, figure 3b, shows that the force compensation is extremely effective at maintaining the desired forward velocity. In contrast, the standard LOS algorithm oscillates with the disturbance velocity, but also oscillates around a velocity below the desired value. This is due to the fact that at some forward velocity the forward drag force becomes balanced with the forward thrust command associated with the velocity error, reaching a false equilibrium state. Therefore, an additional integral control term would be required in (6) in order to reach the desired forward velocity, but this would cause more issues due to the oscillating disturbance forces.The disturbance force compensation algorithm reaches the desired velocity because it compensates for all measured hydrodynamic forces acting on the vehicle, which includes both the force due to the disturbance as well as the drag forces due to vehicle motion.

Figure 4 shows the RMS position error for all the runs with the different disturbance amplitudes. The total error for both strategies is negligible when the disturbance amplitude drops to zero and there is no difference between the performance of the two strategies. As the disturbance amplitude increases, the total error for both control strategies also increases, but the total error for the disturbance force compensation algorithm is noticeably lower. Furthermore, the total error for the standard LOS heading controller grows nearly linearly with the increase in disturbance amplitude, whereas the total error for cases using the force compensation technique level off as the disturbance amplitude increases. This is due to the fact that the vehicle requires some time to adjust it's heading in order to account for the disturbance forces, but the error associated with this delay depends more on the vehicle dynamic properties (i.e. maximum turning rate), so it is less sensitive to the disturbance amplitude. In addition, it can be seen if figure 3 that for the disturbance compensation case the separation distance initially reaches a peak value while the vehicle is turning to compensate, but then slowly decreases before the force has subsided. This further validates the claim that much of the position tracking error is due to limitations in vehicle turning rates.

Figure 5 shows the total RMS error in forward velocity tracking over the same range of disturbance amplitudes with a disturbance frequency of 0.03 Hz. It can be seen that the error for the disturbance compensation cases are nearly constant for all disturbance amplitudes indicating that the forward velocity tracking error is purely due to the initial ramp up to the desired velocity. Furthermore, the total error for the the standard LOS algorithm is nearly double that of the disturbance compensation strategy for the entire range due to the false equilibrium point. Interestingly, the

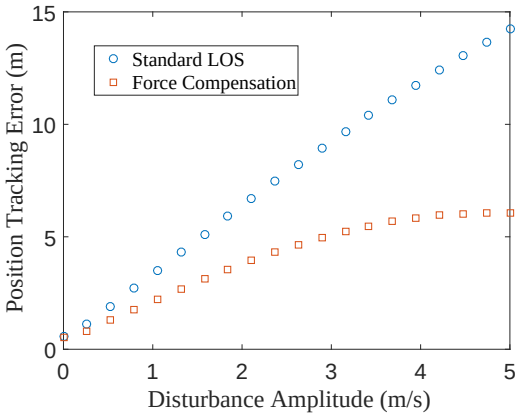

Fig. 4. Total position tracking error of the underactuated vehicle while attempting to follow the WP1 waypoint trajectory, subjected to a range of background disturbance velocity amplitudes, using both a standard LOS trajectory and a disturbance force compensation algorithm. The total error is calculated as the root mean square of the separation distance from the desired path.

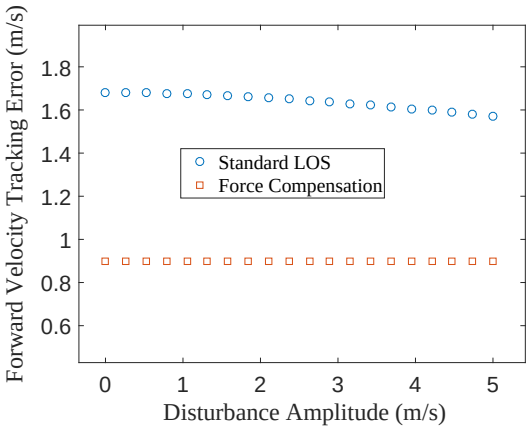

Fig. 5. Total error in forward velocity tracking for the vehicle using both standard LOS heading control and disturbance force compensation control for a range of disturbance amplitudes. The disturbance frequency for all cases in 0.03 Hz.

forward velocity tracking error actually decreases slightly as the disturbance amplitude increases because the oscillation in vehicle velocity due to the influence of the disturbance actually brings the forward velocity closer to the desired value.

Finally we look at the effect on position tracking if the frequency of the fluid disturbance changes. Figure 6 shows the total position tracking error for the two control strategies over a range of disturbance frequencies. For all cases the disturbance amplitude is set to A = 3 m/s. As can be seen in this figure, as the disturbance frequency gets large the total position tracking error asymptotically approaches zero, and the two control methodologies become nearly equivalent. This is due to the fact that at higher frequencies the vehicle inertia prevents significant displacement before the disturbance changes directions. Similarly as the frequency decreases the displacement becomes very large before changing directions causing a large total position

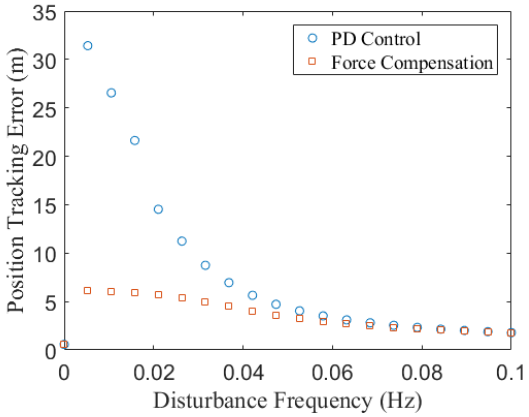

Fig. 6. Total error in forward velocity tracking for the vehicle using both standard LOS heading control and disturbance force compensation control for a range of disturbance amplitudes. The disturbance frequency for all cases in 0.03 Hz.

tracking error for the standard LOS algorithm.

V. CONCLUSIONS

Recent studies have shown excellent potential for a novel control methodology inspired by fish lateral line sensory systems, whereby a vehicle measures exact hydrodynamic forces acting on it via a distributed pressure sensor array, and then applies control forces to instantaneously compensate for measured fluid forces. in order to cancel out the disturbance forces the vehicle must have full control authority in all degrees of freedom. However most marine vehicles are underactuated, and rely on forward propulsion with steering control. We developed a new motion control algorithm, which is a modified line-of-sight heading algorithm, to allow these vehicles to utilize hydrodynamic force measurements and improve position tracking. We demonstrate the effectiveness of the derived control strategy by creating a simulation of an underactuated vehicle in the presence of fluid disturbances, under both a standard line-of-site heading algorithm and the one defined here. The new motion controller significantly reduces position tracking error, especially for low frequency and high amplitude disturbances, 50% in some cases.

As a final note, we should point out that the simulation makes no adjustments accounting for maximum thruster limitations or nozzle rotational speed. We are also not including any possible error in the hydrodynamic force measurement which will degrade performance. Furthermore, if a fully controllable vehicle, with multiple thrusters capable of simultaneously providing forces/torques in all three lateral directions, was simulated under similar constraints; the heading algorithm would not be necessary, and the vehicle would track the waypoint trajectory exactly. For this hypothetical case the tracking error would be improved by at least a factor of three. We will gladly perform more simulations with more realistic parameters if this is desired.

ACKNOWLEDGMENT

This work is supported by a grant from the office of naval research (ONR), and by a grant from the National Science Foundation (NSF)

REFERENCES

[1] G. Antonelli, *Underwater Robots*, ser. 1610-7438. Cham, Switzerland: Springer, 2006, ch. 3, pp. 65–100.

[2] T. I. Fossen, *Guidance and Control of Ocean Vehicles*. Hoboken, NJ, USA: Wiley-Interscience, 1994.

[3] G. Antonelli, F. Caccavale, S. Chiaverini, and L. Villani, "Tracking control for underwater vehicle-manipulator systems with velocity estimation," *IEEE Journal of Oceanic Engineering*, vol. 25, no. 3, pp. 399–413, 2000. [Online]. Available: http://dx.doi.org/10.1109/48.855403

[4] G. Antonelli, S. Chiaverini, N. Sarkar, and M. West, "Adaptive control of an autonomous underwater vehicle: Experimental results on ODIN," *IEEE Transactions on Control Systems Technology*, vol. 9, no. 5, pp. 756–765, 2001. [Online]. Available: http://dx.doi.org/10.1109/87.944470

[5] D. Yoerger and J. Slotine, "Robust trajectory control of underwater vehicles," *IEEE Journal of Oceanic Engineering*, vol. 10, no. 4, pp. 462–470, 1985.

[6] A. J. Healey and D. Lienard, "Multivariable sliding mode control for autonomous diving and steering of unmanned underwater vehicles," *IEEE journal of Oceanic Engineering*, vol. 18, no. 3, pp. 327–339, 1993.

[7] T. I. Fossen and S. I. Sagatun, "Adaptive control of nonlinear systems: A case study of underwater robotic systems," *Journal of Field Robotics*, vol. 8, no. 3, pp. 393–412, 1991. [Online]. Available: http://dx.doi.org/10.1002/rob.4620080307

[8] J. Yuh, "Modeling and control of underwater robotic vehicles," *IEEE Transactions on Systems, Man and Cybernetics*, vol. 20, no. 6, pp. 1475–1483, 1990. [Online]. Available: http://dx.doi.org/10.1109/21.61218

[9] D. B. Marco and A. J. Healey, "Local area navigation using sonar feature extraction and model-based predictive control," *International Journal of Systems Science*, vol. 29, no. 10, pp. 1123–1133, 1998. [Online]. Available: http://dx.doi.org/10.1080/00207729808929602

[10] B. Allotta, A. Caiti, R. Costanzi, F. Fanelli, D. Fenucci, E. Meli, and A. Ridolfi, "A new AUV navigation system exploiting unscented kalman filter," *Ocean Engineering*, vol. 113, pp. 121–132, 2016. [Online]. Available: http://dx.doi.org/10.1016/j.oceaneng.2015.12.058

[11] T. W. Kim and J. Yuh, "A novel neuro-fuzzy controller for autonomous underwater vehicles," in *ICRA*, Seoul, Korea, May 2001, pp. 2350–2355.

[12] P. Walters, R. Kamalapurkar, F. Voight, E. M. Schwartz, and W. E. Dixon, "Online approximate optimal station keeping of a marine craft in the presence of an irrotational current," *IEEE Trans. Rob.*, vol. 34, no. 2, pp. 486–496, 2018.

[13] Y. Xu and K. Mohseni, "Bio-inspired hydrodynamic force feed forward for autonomous underwater vehicle control," *IEEE/ASME Transactions on Mechatronics*, vol. 19, no. 4, pp. 1127–1137, 2013. [Online]. Available: http://dx.doi.org/10.1109/TMECH.2013.2271037

[14] K. Nelson and K. Mohseni, "Design of a 3-D printed, modular lateral line sensory system for hydrodynamic force estimation," *Marine Technology Society Journal*, vol. 51, no. 5, pp. 103–115, 2017. [Online]. Available: https://doi.org/10.4031/MTSJ.51.5.9

[15] M. Krieg, K. Nelson, and K. Mohseni, "Distributed environmental sensing for intelligent mobile robots," *Nature: Machine Intelligence*, vol. Under Review, 2018.

[16] A. J. Healey and D. B. Marco, "Slow speed flight control of autonomous underwater vehicles: Experimental results with the NPS AUV II," in *2nd International Offshore and Polar Engineering Conference*, San Fransisco, CA, USA, 1992, pp. 523–532.

[17] T. Holzhuter and R. Schultze, "On the experience with a high-precision track controller for commercial ships," vol. CEP-4, no. 3, 1996, pp. 343–350.